The Phase Function of Main-Belt Comet P/2008 R1 (Garradd)

Eric MacLennan[1,2], Henry Hsieh[1]

[1]Institute for Astronomy, [2]Northern Arizona University

ABSTRACT

We present observations of the Main-Belt Comet P/2008 R1 (Garradd) allowing the study of the object's phase function. Main-Belt Comets are characterized as having orbits indistinguishable from main-belt asteroids and exhibiting cometary activity. While inactive, images of Garradd were taken by the Gemini North telescope atop Mauna Kea allowing us to measure the absolute magnitude H_R = 20.3 ± 0.1 mag and slope parameter G_R = 0.08 ± 0.05 used in the IAU phase function. Assuming an R-band albedo of p_R = 0.05 we determine an effective radius of $r_N \approx$ 0.22 km. Knowledge of the phase function and radius allows us to look at 2008 observations of Garradd when it was active and quantify dust mass loss.

INTRODUCTION

First identified in 2006 [1], main-belt comets (MBCs) have orbits completely confined to the main asteroid belt, yet exhibit cometary activity indicative of the sublimation of volatile ice. By providing evidence that ice exists in the present-day asteroid belt, they present an invaluable opportunity to evaluate the plausibility of hypotheses that icy main-belt objects may have played a significant role in the primordial delivery of terrestrial water [2].

MBC P/2008 R1 (Garradd) (semimajor axis, a = 2.726 AU; eccentricity, e = 0.342; inclination, i = 15.90°) was the fourth MBC to be discovered and was thoroughly studied by [3] while it was active. [3] estimated a dust production rate of 1.5 kgs^{-1} during its 2008 activity and determined that it was dynamically unstable on timescales of ~ 20 - 30 Myr. This dynamical result indicates that P/Garradd is unlikely to be native to its current location, and is thought to originate elsewhere in the asteroid belt, perhaps in the outer belt where other MBCs are found [3]. An origin elsewhere in the outer solar system, however, cannot be ruled out. Photometry by [3] indicated that the nucleus had an effective radius no larger than r_e < 0.7 km, but since the object remained active throughout their observational campaign, they were unable to ascertain the true nucleus size.

We thank the Research Experience for Undergraduate Program at the Institute for Astronomy supported and funded by the National Science Foundation.

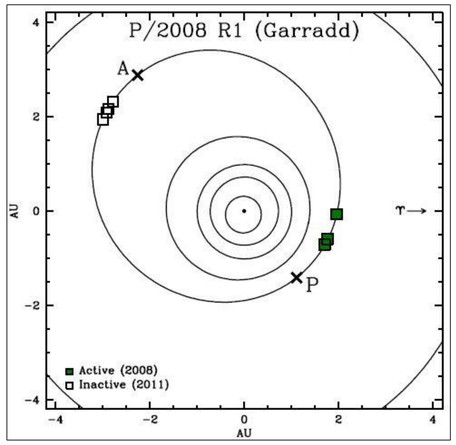

Figure 1. Orbital position plot for Garradd observations described in Table 1 and Table 2. The Sun is shown at the center as a solid dot, with orbits of Mercury, Venus, Earth, Mars, Garradd, and Jupiter (from the center outward) shown as black lines. Green squares mark positions where Garradd was observed to be active in 2008 by [3] and open squares mark inactive positions in 2011. The perihelion (P) and aphelion (A) positions are marked with crosses.

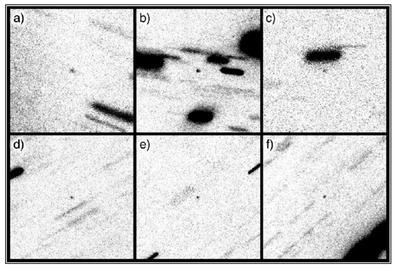

Figure 2. Composite R-band images of Garradd constructed from observations on (a) 2011 February 09 (b) 2011 February 28 (c) 2011 March 11 (d) 2011 March 26 (e) 2011 March 31 (f) 2011 April 1, with total effective exposure times of 1200s, 2400s, 1200s, 1800s, and 1800s, respectively. Garradd is shown at the center of each panel which measures 30" by 30" with North up and East to the left.

OBSERVATIONS

Images were taken using the 8 m Gemini North telescope located at Mauna Kea Observatory in Hawaii. The imaging mode of the Gemini Multi-Object Spectrograph (GMOS), which uses the Sloan Digital Sky Survey g'r'i'z' filters, was used along with non-sidereal tracking along the motion of Garradd in all observations. In this study of Garradd observations were taken when the object has just passed aphelion where it is not suspected to harbor visible dust production. A plot of the locations of Garradd in its orbit when it was observed to be active in 2008 and observations for this study in 2011 are included in Figure 1. Data was collected on six nights between UT 2011 February 5 and 2011 April 1 (Figure 2).

Standard image calibration (bias subtraction and flat-field reduction) was performed for all images. Flat fields were constructed from dithered images of the twilight sky. Absolute calibration of object magnitude was done using a selection of 3 - 8 field stars from the SDSS catalog [4] and a circular aperture around the object ranging from 0". 3 to 0".7, depending on the seeing conditions during each night. We transform our measurements to the BVRI system assuming solar colors, to allow our phase function to be computed in the R-band.

DUST ACTIVITY

Using the parameters obtained from the phase function of Garradd we can estimate the amount of dust that was present in the 2008 observations. The calculated reduced R-band magnitudes are used with the predicted reduced magnitudes to determine the ratio of scattering surfaces of dust, A_d, to that of the nucleus, A_N, using

$$\frac{A_d}{A_N} = \frac{1-10^{0.4(m_{tot}(1,1,\alpha)-m_R)}}{10^{0.4(m_{tot}(1,1,\alpha)-m_R)}} \quad (1)$$

where m_{tot} is the calculated reduced magnitude from [3] when the total flux of Garradd was measured, including dust surrounding the coma, and m_R is the expected reduced magnitude according to the IAU phase function with our newly measured parameters. Using the estimated radius for Garradd in Section 2, a total dust mass can be calculated if we assume a = 10 μm radius grain size with bulk density ρ = 1300 kg m^{-1} [5] by the following:

$$M_d = \frac{4}{3}\rho a \cdot A_N \left(\frac{A_d}{A_N}\right) \quad (2)$$

Dust to nucleus scattering surface ratios and dust mass values derived from the 2008 observations of Garradd are included in Table 1, along with the predicted magnitudes presented in [3].

PHASE FUNCTION ANALYSIS

An objects brightness variation with solar phase angle (phase function) is dependent on the surface properties of the object such as regolith porosity, albedo, particle size-distributions and roughness [6],[7]. Thus an understanding of the phase function parameters for Garradd and other objects provide an approach of comparing the surface properties. Knowledge of the phase function also helps us accurately determine the expected magnitude of the object at any observing geometry, assuming it is inactive.

We compute R-band reduced magnitude (m(1,1,α); i.e. for R = Δ = 1 AU) assuming an $R^{-2}\Delta^{-2}$ inverse square law dependence on brightness. The resulting reduced magnitude is only dependent on the phase angle and any rotational variation of the object. By using sparse sampling, we can partially compensate for the unknown rotational phase of the object and include such variations as source of uncertainty in our final phase function solution.

Best-fitting of the linear phase function to the reduced magnitude of Garradd we find values of $m_R(1,1,0)$ = 20.5 ± 0.1 mag and β = 0.04 ± 0.5 mag deg^{-1}. Additionally, the IAU phase function described in [8] yields best-fit values of H_R = 20.3 ± 0.1 mag and G_R = 0.08 ± 0.05. For comparison, the slope parameters of MBCs 238P, 176P and 133P are G = -0.03 ± 0.10 [9], G = 0.26 ± 0.05 and G = 0.04 ± 0.05 [10], respectively. Using a geometric R-band albedo of p_R = 0.05, measured for other MBCs [10] we estimate an effective nucleus radius of $r_n \approx$ 0.22 km.

UT Date	$m_{tot}(R,\Delta,\alpha)^a$	R^b	Δ^c	α^d	$m_{tot}(1,1,\alpha)^e$	$m_R(1,1,\alpha)^f$	$\frac{A_d\rho a}{A_N}$	M_d^h
Sep 26	19.69 ± 0.05	1.85	1.09	26.5	18.16 ± 0.05	21.61 ± 0.05	23.00	6.17
Sep 30	19.88 ± 0.03	1.86	1.13	27.1	18.28 ± 0.03	21.63 ± 0.03	20.95	5.62
	19.93 ± 0.03	1.86	1.13	27.1	18.33 ± 0.03	21.63 ± 0.03	19.96	5.36
Oct 1	19.86 ± 0.02	1.86	1.13	27.3	18.24 ± 0.02	21.64 ± 0.02	21.86	5.87
Oct 2	19.9 ± 0.03	1.87	1.14	27.4	18.26 ± 0.03	21.64 ± 0.03	21.50	5.77
Oct 3	20.17 ± 0.06	1.86	1.15	27.6	18.51 ± 0.06	21.65 ± 0.06	16.94	4.55
Oct 22	21.09 ± 0.04	1.91	1.33	29.5	19.06 ± 0.04	21.70 ± 0.04	10.44	2.80
Nov 11	21.21 ± 0.10	1.97	1.56	30.0	18.78 ± 0.10	21.72 ± 0.10	14.05	3.77

Table 1. Photometric Excess from [3]. (a) Total observed magnitude of Garradd reported in [3] in a 2".2 radius Aperture (b) Heliocentric distance in AU (c) Geocentric distance in AU (d) Solar phase angle (Sun-Garradd-Earth) in degrees (e) Total reduced magnitude of Garradd (f) Expected reduced magnitude from IAU phase law (g) Dust-to-Nucleus scattering surface (h) Dust mass loss in 10^4 kg.

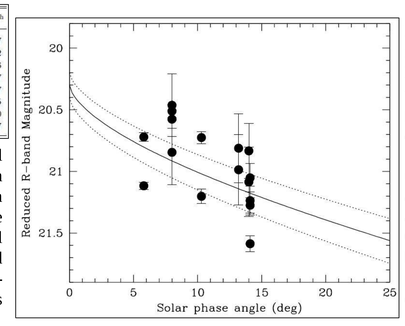

Figure 3. Phase function solution for P/2008 R1 Garradd with the best-fit IAU phase law plotted as a solid line. Dotted lines show the uncertainty in absolute magnitude and slope parameter. Observed reduced R-band magnitudes are plotted as solid circles.

DISCUSSION

Based on the magnitude measurements of Garradd on the nights of March 31, 2011 and April 1, 2011 the photometric range for the object is > 0.8 mag. This value, along with a rotation period, can be constrained by further, more comprehensive observations of Garradd while it remains inactive.

Currently, most MBCs consistently show activity only near perihelion [9], thus it is important to monitor Garradd during its next perihelion passage in January 2013. Observations of further dust loss will confirm that Garradd's activity is cometary and driven by the sublimation of water ice at or beneath the surface. The range of activity over next perihelion can be measured, and compared to other MBCs to investigate the driving mechanism behind cometary activity.

CITATIONS

[1] Hsieh, H.H., & Jewitt, D. 2006, Science, 312, 561-563. [2] Morbidelli, A., Chambers, J., Lunine, J.I., Petit, J.M., Robert, F., Valsecchi, G.B., & Cyr, K.E. 2000, Meteoritics & Planetary Science, 35, 1309-1320. [3] Jewitt, D., Yang, B., & Haghighipour, N. 2009, AJ, 137, 4313. [4] York et al. 2000, AJ, 120, 1579. [5] Hsieh, H.H., Jewitt, D., & Fernandez, Y. R., 2004, AJ, 127, 2997. [6] Helfenstein, P., & Veverka, J. 1989, Asteroids II. University of Arizona Press, Tucson, p. 557. [7] Muinonen, K., Piironen, J., Shkuratov, Y.G., Ovcharenko, A., & Clark, B.E. 2002, Asteroids II. University of Arizona Press, Tucson, p. 123. [8] Bowell E., Hapke B., Domingue D., Lumme K., Peltoniemi J., Harris A. W., 1989, Asteroids II. University of Arizona Press, Tucson, p. 524. [9] Hsieh, H.H., Meech, K., & Pittichova, J., 2011, ApJ, 736, L18. [10] Hsieh, H.H., Jewitt, D., & Fernandez, Y. R., 2009, ApJ, 694, L111.